Evolutionary genomics of sex-related chromosomes at the base of the green lineage 2

L Felipe Benites, François Bucchini, Sophie Sanchez-Brosseau, Nigel Grimsley, Klaas Vandepoele, Gwenael Piganeau

Evolutionary genomics of sex-related chromosomes at the base of the green lineage

L. Felipe Benites[1,a], François Bucchini[2,3,a], Sophie Sanchez-Brosseau[1], Nigel Grimsley[1], Klaas Vandepoele[2,3,4], Gwenaël Piganeau[1*]

Author affiliations:

[1]Integrative Biology of Marine Organisms (BIOM), Sorbonne University, CNRS, Oceanological Observatory of Banyuls, Banyuls-sur-Mer, France

[2]Ghent University, Department of Plant Biotechnology and Bioinformatics, Technologiepark 71, 9052 Ghent, Belgium

[3]VIB Center for Plant Systems Biology, Technologiepark 71, 9052 Ghent, Belgium

[4]Bioinformatics Institute Ghent, Ghent University, Technologiepark 71, 9052 Ghent, Belgium

[a] equal contribution

[*] **Corresponding author:** gwenael.piganeau@obs-banyuls.fr

Keywords : recombination suppression, mating-type loci, chlorophyta, GC content phylogenetic profiling

Abstract

While sex is now accepted as a ubiquitous and ancestral feature of eukaryotes, direct observation of sex is still lacking in most unicellular eukaryotic lineages. Evidence of sex is frequently indirect and inferred from the identification of genes involved in meiosis from whole genome data and/or the detection of recombination signatures from genetic diversity in natural populations. In haploid unicellular eukaryotes, sex-related chromosomes are named mating-type (*MT*s) chromosomes and generally carry large genomic regions where recombination is suppressed. These regions have been characterized in Fungi and Chlorophyta and determine gamete compatibility and fusion. Two candidate *MT*+ and *MT*- alleles, spanning 450-650 kb, have recently been described in *Ostreococcus tauri*, a marine phytoplanktonic alga from the Mamiellophyceae class, an early diverging branch in the green lineage.

Here, we investigate the architecture and evolution of these candidate *MT*+ and *MT*- alleles. We analysed the phylogenetic profile and GC content of *MT* gene families in eight different species, whose divergence has been previously estimated at up to 640 million years, and found evidence that the divergence of the two *MTs* alleles predates speciation in the *Ostreococcus* genus. Phylogenetic profiles of *MT* trans-specific polymorphisms in gametologs disclosed candidate *MTs* in two additional species, and possibly a third. These Mamiellales *MT* candidates are likely to be the oldest mating-type loci described to date, which makes them fascinating models to investigate the evolutionary mechanisms of haploid sex determination in eukaryotes.

keywords: sex determining chromosome, recombination suppression, mating types, Chlorophyta, Mamiellophyceae

Significance statement:

Direct evidence of sexual reproduction is difficult to observe in many unicellular eukaryotes, while indirect evidence relies on gene content or recombination signatures. Here we report the gene content of two candidate mating type loci in a unicellular phytoplanktonic eukaryote. Identification and phylogenetic analyses of the gametologs shared between the two mating types suggest signatures of trans-specific evolution, i.e. an ancient divergence, prior to the speciation events within the Ostreococcus lineage. The divergence between gametologs can be leveraged to assign strains from distantly related species to each of the two mating types. Thus, they are likely to be the oldest mating-type loci described to date, which makes them

fascinating models to investigate the evolutionary mechanisms of haploid sex determination in eukaryotes.

Introduction

Meiotic sex and its associated intra-chromosomal and inter-chromosomal recombination events are considered ubiquitous, ancestral features of eukaryotes (Speijer et al. 2015). Across the eukaryotic tree of life, meiotic sex has been reported in many algal lineages (reviewed in Umen and Coelho 2019), such as chlorophytes (Sager and Granick 1954; Suda et al. 1989; Fučíková et al. 2015), bacillariophytes (Chepurnov et al. 2004), chlorarachniophytes (Beutlich and Schnetter 1993), cryptophytes (Hill and Wetherbee 1986; Kugrens and Lee 1988), cyanidiophytes (Malik et al. 2007), dinoflagellates (Pfiester 1989) and euglenoids (Ebenezer et al. 2019).

There have been intense efforts to study sex determining mechanisms and underlying genetic make-up in multicellular animals and plants (Bachtrog et al. 2014 for a review). However, less is known about sex-determining mechanisms in microbial eukaryotes. Ancestral sex-determining mechanisms have evolved in unicellular eukaryotes, so that "*it is clear that the evolution of different sexes in its most basic form is represented by the evolution of mating-types*" (Hoekstra 1987). Obviously, it is less straightforward to identify morphological differences between sexes in microorganisms than in macro-organisms. The term "mating type" describes different "sexual types" in unicellular eukaryotes, and was first coined by Tracy Sonneborn. He used this term to indicate that only certain lines (or "stocks") of the ciliate *Paramecium aurelia* mated with each other, but never with themselves (Sonneborn 1937). He noted that the Paramecium mating system was "*strikingly similar to the sexual differences between gametes in some of the unicellular green alga*". He referred to earlier work by Strehlow (1929) on *plus* and *minus* "*sexes"* reported in unicellular soil and freshwater green algae from the order Chlamydomonadales. In the Fungal kingdom, there has been a rapidly growing experimental evidence of mating types for many species (reviewed in Billiard et al. 2012; Wolfe and Butler 2017), initially in the yeasts *Saccharomyces cerevisiae* (Astell et al. 1981) and *Neurospora crassa* (Staben and Yanofsky 1990). Mating types were identified later in the green algal lineage, as in *Chlamydomonas reinhardtii* (Ferris et al. 2002), and across the eukaryotic tree of life (reviewed in Umen and Coelho 2019). Interestingly, the evolutionary link between mating types and male and female sexes has been unambiguously demonstrated in the volvocine green lineage (Nozaki et al. 2006)(Ferris et al. 2010)(Hamaji et al. 2018). However, the origin of mating-types remains unresolved. Three main hypotheses have been formulated for the origin and maintenance of this genetic setup, which requires outcrossing. First, it may mediate the prevention of genetic conflicts (Hurst and Hamilton 1992); second, the prevention of

haploid selfing, that is mating among clonal cells e.g. (Billiard et al. 2011)(Billiard et al. 2012). A third proximate hypothesis is that this genetic system has evolved from a cell signalling system for partner recognition and pairing by producing recognition/attraction molecules and their receptors, as initially suggested by Hoekstra (Hoekstra 1987) and expanded by Hadjivasiliou and Pomiankowski (2016). Common themes of mating-type loci were quickly noticed: they often come in two types (with notable exceptions in Fungi e.g. Billiard et al. (2011) for a review) with hardly any sequence conservation. While orthologous genes may be identified between the two mating-type regions, gametologs, mating type regions share little synteny as a consequence of rearrangements and insertion of repetitive DNA (Ferris and Goodenough 1994; Lengeler et al. 2002; Ferris et al. 2010; Badouin et al. 2015; Fontanillas et al. 2015; Hamaji et al. 2016; Geng et al. 2018). Moreover, mating-type loci may also experience recombination suppression both in diploid sexual system, as well as in haploid sexual systems and the UV sex chromosomes (Bachtrog et al. 2011)(Coelho et al. 2018). Recombination suppression may be stepwise and thus generate 'evolutionary strata' of differentiation between the two mating types (Hartmann et al. 2021 for a review in Fungi). The consequence of recombination suppression are manifold (Charlesworth and Charlesworth 2000) (Charlesworth 2016) and may include a higher probability of fixation of deleterious mutations, massive rearrangements, which may be associated to lower gene density (Yamamoto et al. 2021), GC composition changes, as well as differential gene expression . GC composition results from the balance between mutation biases, selection and GC biased gene conversion (Galtier et al. 2001), a molecular process linked to recombination. Therefore, regions with suppressed recombination are expected to display a significant lower GC content as compared to recombining regions, and a 4 to 10% lower GC content over the mating type locus has been reported in the mating type region of four species of volvocine algae (Hamaji et al. 2018).

The genomic features associated to mating type regions may thus guide the identification of candidate mating type loci in lineages in which genomic data is available, while the experimental conditions eliciting syngamy and meiosis have not yet been found, precluding experimental validation. While there is no direct evidence of sexual reproduction in the cosmopolitan marine picoeukaryote *Ostreococcus tauri* (Mamiellophyceae, Chlorophyta) there are three lines of indirect evidence for sexual reproduction (Grimsley et al. 2010). The first line of evidence comes from screening the whole genome sequence for genes encoding proteins involved in meiosis. These proteins have been described in all Mamiellophyceae species for which full genomes sequences are available, including *O. tauri* (Derelle et al. 2006), *O. lucimarinus* (Palenik et al. 2007), *Micromonas pusilla*, *M. commoda* (Worden et al. 2009), and

in *Bathycoccus* spp. metagenomes from the Arctic (Joli et al. 2017). The second line of evidence comes from population polymorphism data that indicate inter-chromosomal and intra-chromosomal recombination (Grimsley et al. 2010). Indeed, when sequencing can be performed in several strains from the same population, analyses of the polymorphism spectrum allow the estimation of the frequency of sex in natural populations (Tsai et al. 2008; Grimsley et al. 2010; Drott et al. 2020; Hasan and Ness 2020; Koufopanou et al. 2020). Finally, the third line of evidence comes from a population genomic analysis that demonstrated the existence of a candidate mating type loci (450 and 650 kb) in *O*. *tauri* (Grimsley et al. 2010). *O*streococcus *tauri* RCC4221 was suggested to represent the candidate *minus* mating type (hereafter *MT*-) together with *O*. *lucimarinus* CCE9901, because of the presence of a gene encoding for a plant-specific transcription factor from the RWP-RK gene family (Worden et al. 2009). This gene family includes the "sex determining gene" (minus dominance *MID*) of minus mating type loci in Volvocales algae (Ferris and Goodenough 1997; Umen 2011). The candidate opposite mating type (hereafter *MT*+) was identified from the genome analysis of 12 *O*. *tauri* strains lacking sequence homology with *O*. *tauri* RCC4221 over the 650 kb region. These strains also lacked a gene containing an RWP-RK domain (Blanc-Mathieu et al. 2017). Phylogenetic analysis of five gametologs revealed that *O*. *tauri MT*- and *MT*+ genes clustered with different *Ostreococcus* species of the same mating type, respectively. This suggests that mating type differentiation predates speciation within *Ostreococcus*, suggesting that *Ostreococcus MT*+ and *MT*- are remarkably ancient. However, the total number of gametologs, their synteny and sequence conservation among Mamiellales and Mamiellophyceae remains unknown.

Here, we investigated the architecture and phylogenetic profiles of the *MT*+ and *MT*- alleles to unfold their evolutionary history. We analyzed the gene set of the two candidate mating type loci, and identified the complete set of gametologs between them. This allowed us to define the set of orthologous genes located inside each of the available candidate *MT* loci in Mamiellales. This dataset was then leveraged (i) to investigate the presence of evolutionary strata, (ii) construct gene genealogies to search for trans-specific evolution signatures (iii) identify the opposite mating types from additional Mamiellophyceae sequence data. This allowed to trace back the age of the divergence of the *MT*+ and *MT*- alleles in this early diverging branch of the green lineage.

Results

Sorting out gene families in *O. tauri MT* according to their prevalence across species

The GC content can be used as a predictor of recombination rates in genomes undergoing GC-biased gene conversion (e.g. Meunier and Duret 2004; Charlesworth et al. 2020), and it was suggested that there is an inverse relationship between chromosome length and GC content, which is consistent with GC biased GC conversion in *Ostreococcus* (Jancek et al. 2008). The genome-wide spontaneous mutation rate is GC->AT biased, which is consistent with a mechanism like GC-biased gene conversion that could explain the difference between the observed 0.60 GC frequency in the genome and the expected equilibrium 0.36 GC frequency under mutation bias (Krasovec et al. 2017). The detection of the sharp (~9 to 17%) decrease in GC content on the big outlier chromosome was used to define *MT* boundaries in *O. tauri* RCC4221 (*MT*-), *O. tauri* RCC1115 (*MT*+), and six Mamiellales genomes (Figure 1, supplementary table S1, Supplementary Material online). Using OrthoFinder, we assigned genes from the *Ostreococcus* spp., *Bathycoccus prasinos*, *Micromonas commoda,* and *Micromonas pusilla* to gene families (GFs). Mating type gene families were defined as GFs with members located within the *MT* region of either *O. tauri* RCC4221 (*MT*-) or *O. tauri* RCC1115 (*MT*+). The presence/absence of the genes of these GFs in the lineage provides important information about *MT*+ and *MT*- specific GFs, as well as four additional distinct non-overlapping GF categories (table 1).

Table 1: Classification, description, and quantities of genes and gene families (GFs) in *O. tauri* RCC4221 *(MT-)* and RCC1115 (*MT+*) strains.

Gene Family class	Features of included genes	RCC4221 (*MT-*)	RCC1115 (*MT+*)
MT specific GFs	Present in either all *Ostreococcus MT-* or all *Ostreococcus MT+*	6 genes in 6 GFs	2 genes in 2 GFs
Core *MT* GFs	Present in all Mamiellales genomes and located only in *MT* region	23 genes in 23 GFs	23 genes in 23 GFs
Shared *MT* GFs (non-core)	Present in both *Ostreococcus MT* loci, but not in all Mamiellales *MT* regions	75 genes in 69 GFs	79 genes in 69 GFs
GFs extending outside *MT*	Present in one *Ostreococcus MT* locus but with homologous genes in other regions in the opposite strain	28 genes in 27 GFs	8 genes in 4 GFs
GFs not retained for analysis	Present in only one *Ostreococcus MT* locus and Mamiellales genomes but absent from the genomes of the opposite strains/*MT*; divergent GFs or singletons	112 genes	128 genes
Total number of genes		244	240

The "*MT* specific" GF class contains genes that are shared only by *Ostreococcus* genomes from the same *MT*. The *MT*-specific GFs contain the smallest number of genes: 6 and 2 genes for *MT-* and *MT+*, respectively. These GFs are expected to contain genes involved in sex determination and functional control associated with each *MT*, as well as dispensable genes trapped into this locus (Wilson et al. 2019 for a review in Ascomycetes). Functional annotation revealed that most of these genes encode for hypothetical proteins or do not have any predicted function. The *MT-* specific GFs contain a gene with an RWP-RK domain (ostta02g01710), as previously reported (Worden et al. 2009), and a gene (ostta02g00990) that encodes for an SRP-dependent co-translational protein involved in targeting proteins to the membrane. Within the *MT+*-specific GFs, there are only 2 genes, which encode for hypothetical proteins annotated with Gene Ontology terms linked to mismatch repair, protein binding, and transport (supplementary table S2, Supplementary Material online).

The "core *MT*" GF class contains GFs exclusively composed of gametologs that are located inside the boundaries of all candidate *MT* regions in all eight Mamiellales genomes (supplementary table S1, Supplementary Material online). There are 23 "core *MT*" GF, which make up less than 10% of genes of the *MT* (Table 1) and these likely belonged to the ancestral locus which evolved into a *MT* in the lineage. Functional annotation indicates that these genes have housekeeping functions, such as ATP and DNA binding, transcription, glycolipid biosynthesis, protein transport, and RNA methylation, but no obvious link to mating (supplementary table S3, Supplementary Material online).

The largest GF class (69 GFs) regroups gametologs that are shared by both *Ostreococcus MT* loci, and that can be absent from the *MT* regions in some Mamiellales species

(Shared *MT* GFs, non-core). A fourth class of GFs contains genes located within the *O. tauri MT* locus or on standard chromosomes (GF extending outside *MT*), and provides evidence of translocations between standard chromosomes and the MT loci. The remaining GFs are present in only one *O. tauri MT* locus and other Mamiellales genomes, or contain genes that are too divergent to generate phylogenies, as the alignments are too short. Therefore, they were excluded from further analyses, together with singleton genes (except the *MT*-specific GFs).

While the core and specific GFs categories should contain the most ancient genes on the *MT*, the other GF categories likely reflect gain, loss, and translocation of genes in and out of the *MT*. This prompted us to undertake synteny and phylogenetic profiling of each GF to understand its evolutionary dynamics.

Genomic architecture of *O. tauri* mating type regions

Syntenic regions outside the MT loci have been reported between species of the same genus : *O. tauri* and *O. lucimarinus* (Palenik et al. 2007), *M. pusilla* and *M. commoda* (Worden et al. 2009). Within *O. tauri*, regions outside the *MT* locus have been shown to be perfectly syntenic and share >99% nucleotide identity, in sharp contrast with the *MT* region (*O. tauri* Chromosome 2, fig. 1), which cannot be aligned at the nucleotide level between *MT*- (RCC4221) and *MT*+ (RCC1115) (Blanc-Mathieu et al. 2017). We further investigated the relative position of orthologous genes in the *MT*+ and *MT*- regions, but found no evidence for synteny in genes from shared and core GFs between both regions (fig. 2A): *MT* specific genes do not cluster but are interspersed throughout the *MT*+ and *MT*- loci.

Ancient inversion events are a well-known trigger for suppression of recombination in genome evolution, but the relative position of orthologous genes in *MT*- and *MT*+ regions provide no evidence of a past inversion event. Instead, visual examination of the global pattern suggested a large translocation of the [b,c] segment in 5' followed by the [a,b] segment in 3' (fig. 2A). To investigate this hypothesis, we defined a simple statistic, *Sdist*, based on the relative distance between orthologous genes on the *MT*+ and *MT*-: *Sdist* is equal to 0 for perfect co-linearity (see methods). Random permutations of the gene orders enabled the estimation of the null distribution. The observed *Sdist* was not significantly different from the average *Sdist* for orthologous genes placed randomly on the two *MTs* (10,000 permutations, $p > 0.10$). However, the translocation of the 5' extremity of *MT*- (segment [b,c]) to the start of *MT*- (arrow on fig. 2A) was associated with a significantly smaller *Sdist* than the random *Sdist* (100,000 permutations p=0.0054). This demonstrates that this translocation significantly improves the

overall co-linearity between *MT*+ and *MT*-, supporting the idea of a past large-scale translocation in one of the *MT* loci.

To track gene translocation events between the *MT*s and the autosomal regions, we located the positions of 46 (*MT*-) and 30 (*MT*+) genes from GFs sharing genes inside and outside the *MT* regions. Genes of the same GFs as *MT*- genes were located on diverse autosomes (fig. 2B). We also observed a similar patchy distribution for GFs of gene members extending outside the *MT*+ (fig. 2C). This provides evidence for past gene translocations between many autosomes and the *MT* regions.

To search for evidence of evolutionary strata, defined as discrete regions containing orthologous genes with similar substitution rates (Lahn and Page 1999), we computed the rate of synonymous substitutions (Ks) (Tzeng et al. 2004) of the genes belonging to the 69 shared *MT* GFs on *MT*- and *MT*+ in *O. tauri* (shared GFs). We were able to compute the number of non-synonymous substitutions (Ks) for only 22 gene pairs, given that for other gene pairs Ks values were close to saturation. From these 22, 19 had a Ks < 1, and only 2 were adjacent on both the *MT*+ and the *MT*- (supplementary table S4, Supplementary Material online). This is consistent with a scenario of independent gene conversion events between the two *MT*s, except for one event spanning two genes. Interestingly, within these recently diverged genes, only 2 pairs were adjacent in only one of the mating types (*MT*+). This suggests that the source or the destination of the conversion events between *MT*s tends to span several kb. These observations indicate an absence of evidence for strata throughout the large *MT* regions of *O. tauri*. However, this absence of evidence may be reconsidered in the future if additional genome data in novel species can be informative to infer the ancestral gene order on the mating type (Branco et al. 2017).

Phylogenetic insights into evolutionary dynamics of mating types

The topology of each GF phylogenetic tree is informative about the relative chronology of the speciation and the divergence events between the *MT*+ and *MT*- alleles. We assessed whether the topology supported either of the two scenarios: (i) in the "*mating type allele diverged post speciation*" scenario: mating type alleles diverged after speciation events within *Ostreococcus* (no mating type alleles = Post); or (ii) in the "*mating type allele diverged ante speciation*" scenario: mating type alleles diverged prior to the speciation event (mating type allele separation = Ante). This later scenario has previously been coined as trans-specific evolution resulting from long term balancing selection (Richman 2000). Consequently, the variation within the genes following the "Ante" scenario may be named trans-specific

polymorphisms (Devier et al. 2009). The number of GFs for each topology is displayed in fig. 3. Interestingly, this dual phylogenetic signal (mating type allele divergence ante versus post-speciation) is mirrored by a GC3 content signature of the genes. Indeed, genes belonging to GFs that support ancient mating type origin have a significantly lower GC3 content than genes whose evolutionary history is concordant with the speciation history of the genus. For the 23 core *MT* GFs (listed in supplementary table S3, Supplementary Material online), the majority of phylogenies (21 trees, supplementary fig. S1, Supplementary Material online) support the "ancient mating type" evolutionary scenario that mating type region diverged before the speciation events within *Ostreococcus*, whereas only two phylogenies support the scenario of a mating type differentiation after the speciation events.

Thus, most core and shared *MT* GFs support an ancient mating type origin (fig. 4A with mating type separation and 3B without mating type separation). In contrast, the phylogenies of most GFs containing paralogous genes outside the *MT* region are consistent with the speciation tree, suggesting their translocation inside the *MT* locus occurred recently.

Expanding the number of Mamiellales species with two mating type alleles

Since the core *MT* GFs allow *MT+* and *MT-* delineation in the Mamiellales, we used the sequence data to screen 33 transcriptomes (MMETSP and 1KP datasets) from several Mamiellophyceae species for homologous sequences (listed in supplementary table S5, Supplementary Material online). The taxonomic affiliation of each transcriptome was inferred from 18S rDNA sequences (supplementary table S6 and supplementary fig. S2, Supplementary Material online). The phylogenetic range of the transcriptomes spanned from the early divergent freshwater species, such as *Monomastix opisthostigma* (Monomastigales), *Crustomastix*, and *Dolichomastix* (Dolichomastigales), to early Mamiellales, such as *Mantoniella.* It also included several *Micromonas* strains from novel species, such as *M. bravo* and *M. polari*s. In total, at least one homologous gene was recovered for each GF (with an average of 11 GFs per transcriptome) in 28 of 33 transcriptomes (fig. 5).

The most striking pattern came from *O. mediterraneus* MMETSP0929 (strain RCC2572) and *O. lucimarinus* MMETSP0939 (strain BCC118000) transcriptomes. While both datasets displayed hits for almost all core genes (17 out of 23), the taxonomic affiliation inferred for these genes by best blast hit (BBH) was not consistent with the 18S taxonomic affiliation. Instead, it suggested affiliation to a different species of the opposite mating type (supplementary fig. S3, Supplementary Material online). In *O. mediterraneus* MMETSP0929, 14 of 17 genes were affiliated to species from the opposite *MT* groups (*MT*-), such as *O. tauri* and *O. lucimarinus*, not to the reference genome *O. mediterraneus* RCC2590 *MT*+. Likewise, 15 of 17 best blast hits of *O. lucimarinus* MMETSP0939 came from *MT*+ genomes, and not from the *MT*- *O. lucimarinus* reference genome. To confirm the taxonomic affiliation of these genes, we built maximum likelihood phylogenies, including homologs extracted from the transcriptomes (supplementary fig. S3, Supplementary Material online). From the 17 gene families with a best blast hit, 12 passed the alignment length and identity thresholds (see methods). Of these, 10 phylogenies included both *O. mediterraneus* MMETSP0929 and *O. lucimarinus* MMETSP0939, and two phylogenies included only *O. lucimarinus* MMETSP0939. From these, 11 phylogenies were consistent with ancient *MT*+ and *MT*- divergence (example in fig. 6A), while one phylogeny regrouped genes according to species (fig. 6B).

These phylogenetic analyses confirmed the taxonomic affiliation inferred from amino-acid sequence conservation and support an ancient divergence of genes from two *MT* regions. This led us to conclude that *O. lucimarinus* strain RCC2572 and *O. mediterraneus* strain BCC118000 (MMETSP0929 and MMETSP0939, respectively) are of the opposite mating type to the strains for which the reference genome is available. This extends the evidence of the existence of two mating types in *O. tauri* to two additional *Ostreococcus* species.

Identification of candidate mating types based on gene genealogies in *Micromonas commoda*

Micromonas is the most represented Mamiellophyceae genus in the available transcriptomic datasets, with 14 transcriptomes. Therefore, we further examined the individual GF phylogenetic topologies and sequence similarities by using the core *MT* GF set (23 GFs) to search for clustering that might suggest an ancient divergence of *MTs* in *Micromonas*. To this end, we selected *Micromonas* transcriptomes with more than one positive hit with the GFs, and the highest number of hits in the majority of transcriptomes (9 transcriptomes), together with one outgroup from the genus (*Mantoniella* sp. MMETSP1468). Finally, we built individual GF phylogenies from these sequences and the core genes GF dataset (supplementary fig. S4, Supplementary Material online).

A consistent sub-clustering of strains within the *Micromonas commoda* group was observed. MMETSP 1084, 1387, 1403, and 1400 clustered together in 11 of 13 phylogenies, while MMETSP1404 and 1393 clustered with genes from the reference genome of *M. commoda* RCC299 (fig. 7A and supplementary fig. S4, Supplementary Material online). In only two phylogenies, there was no apparent sub-clustering (fig. 7C). Additionally, the branch lengths of the 11 phylogenies displaying sub-clustering were longer and similar to the branch lengths separating *M. polaris* from *M. bravo*, or *M. commoda* from *M. pusilla*. Consistent with this, the average pairwise amino-acid identities between *M. commoda* genes from the two different sub-clusters ranged from 65% to 89% (supplementary table S7, Supplementary Material online). For comparison, we built phylogenies of the actin and β-tubulin genes (fig. 7B and 7D), which are highly conserved, and their phylogenetic topology showed a species topology signature, where these strains did not support two sub-clusters. Pairwise amino-acid identity for the latter GFs between strains ranged from 98% to 99.4% (for actin and β-tubulin, respectively), as expected for strains from the same species. This phylogenetic signal was similar to the *Ostreococcus* core GF phylogenies, consistent with an ancient mating type separation (fig. 4A). Despite the low number of genes (13 genes from 23 GFs), this sub-clustering suggests that there are two *MTs* in *Micromonas commoda*: strains MMETSP1404, 1393, and *M. commoda* RCC299 (the reference genome); and strains MMETSP 1084, 1387, 1400, and 1403, representing the opposite *MT*. As Worden et al. (2009) suggested, *M. commoda* RCC299 would represent the *MT*-, given the presence of an RWP-RK motif gene in its candidate *MT* region. Thus, the strains MMETSP 1084, 1387, 1403, and 1400 would represent the *MT*+ type. Taken

together, phylogenetic analyses of GFs are consistent with an ancient gene divergence of *MT* gametologs in the *M. commoda* lineage, as expected under recombination suppression.

Clues about earlier origin of Mating Type loci in Mamiellophyceae

As the phylogenetic signal may be lost over time as a consequence of the decay of similarity between orthologs (Jain et al. 2019), we investigated indirect signatures of *MTs*. *MT*s evolve without recombination, and this has been shown to decrease GC content. We therefore investigated whether a GC signature could be detected in homologous genes to the core GFs outside the Mamiellales (comprising *Ostreococcus*, *Bathycoccus* and *Micromonas*). Thus, we analysed the GC content of the synonymous third codon position (GC3) of core GF hits in several Mamiellophyceae species, and compared this to the GC3 content of genes from the background genome or transcriptome**.** Core *MT* GFs have significantly lower GC3 (around 20%) than genes of the background genome (or transcriptome) in *Bathycoccus*, *Ostreococcus* and *Micromonas* (fig. 8 and supplementary table S8, Supplementary Material online). Interestingly, we found evidence of a similar difference in GC3 content between gene hits against the core *MT* GFs and the background transcriptome in *Mantoniella squamata* CCAP 1965/1 and the uncultured Mamiellophyceae (uncultured eukaryote RCC2288), with ~10% and 20% differences between genes from the GFs and genes from the background transcriptome, respectively. This suggested that genes that are homologous to the core GFs are also located in a low GC chromosome region in these Mamiellophyceae species (fig. 8 and supplementary table S8, Supplementary Material online). However, there is no evidence for a GC3 content difference between homologous genes to the core GFs and the genes from the background transcriptome in *Crustomastix or Monomastix* (fig. 8).

Discussion

Direct evidence of meiosis is not available for most marine planktonic microbial eukaryotes. This is either due to the difficulty in culturing certain species, or because experimental studies are hampered by a lack of knowledge about sex determination and the conditions required to induce a sexual cycle. In the case of haploid green picoalgae (cell diameter < 2 µm) of the Mamiellales lineage, population genomics data in one species allowed the identification of two candidate mating type alleles with suppressed recombination (Blanc-Mathieu et al. 2017). Here, comparative genomics of seven related species within the Mamiellales lineage unravelled different facets in the mode and tempo of evolution in this enigmatic locus.

First, while no *MT*+ and *MT*- specific genes could be identified for all seven species, *MT*+ and *MT*- specific genes could be identified within the *Ostreococcus* genus. *MT*- specific genes may be implicated in mating type differentiation, such as the previously identified gene encoding an RWP-RK domain (Worden et al. 2009). The two *MT*+ specific genes that have been identified in *Ostreococcus* encode for unknown proteins. One of these proteins (gm1.767_g) harbours WD40 repeats and is predicted to bind to other proteins. The second protein has a DNA binding domain, which is also found in DNA mismatch repair proteins (gm1.689_g, PF00488). A WD40 protein has been shown to regulate mating in the fungus *Ustilago maydis* (Wang et al. 2011). Nevertheless, the functional range of WD40 proteins is too wide to confidently infer a role of the *Ostreococcus* protein to act as a *MT*+ signal protein.

Second, comparative phylogenetics of core gametologs allowed the identification the opposite mating types in two additional species for which transcriptomes were available: the *MT*- in *O. mediterraneus* and the *MT*+ in *O. lucimarinus*. This mating type profiling is made possible by the high divergence between the *MT*+ and *MT*- regions, as gametologs cluster by *MT* and not by species. By screening available environmental data from the TARA Oceans project for the presence of these gametologs, we previously found that, in fact, both mating types of *O. lucimarinus* were present at the stations where this species had been detected (Leconte et al. 2020). Mating type profiling was also suggested between strains from *M. commoda:* phylogenies of the gametologs suggest two clusters of strains, in contrast with phylogenies of highly conserved housekeeping genes (actin, β-tubulin, and 18s rDNA) (fig. 7; supplementary table S7 and supplementary fig. S2, Supplementary Material online).

Third, analysing additional transcriptome data from early diverging branches of the Mamiellophyceae class, we could detect orthologous genes to the Mamiellales gametologs in

eight additional transcriptomes. However, we could not detect any significant difference in GC3 signatures in the earliest Mamiellophyceae, as would be expected under suppressed recombination; on the contrary, GC3 values appear to be higher in homologous genes in Dolichomastigales. This suggests the Mamiellales gametologs are not part of a lower GC region in earlier branching Mamiellophyceae. The conservation of 23 gametologs within the Mamiellales lineage prompted us to investigate the dynamic of these genes. The additional gametologs within the *Ostreococcus* lineage support an ancient large translocation event. Inversions have been previously suggested to trigger recombination suppression and have been recently reported in the origin of a young sex-determining chromosome (Natri et al. 2019). However, translocations are also expected to disrupt recombination (McKim et al. 1988).

One intriguing feature of sex determining chromosomes is their organization as multiple discrete regions, where genes can be clustered by genetic divergence (measured by the rate of non-synonyms substitutions), defined as "evolutionary strata". In humans, strata were first described by Lahn and Page (1999), who suggested that suppression of recombination was initiated in one region (stratum) and later expanded in discrete steps, by strata. This could happen through additional chromosomal inversions, which are known to suppress recombination in mammalian chromosomes. Only a few X-Y sequence similarities persist, and these alleles are orderly stratified by age in the X chromosome and scrambled in the Y. Although strata have been observed in several vertebrates, plants, and fungi (Bachtrog et al. 2014; Badouin et al. 2015; Coelho et al. 2018), they do not appear to be a common feature of algal mating types and sex chromosomes. Indeed, we found no evidence of evolutionary strata in *Ostreococcus MT*s, as neither ancient nor recent genes cluster in any of the *MT*s This may be due to their ancient divergence, associated with a limited more recent expansion dynamic, as suggested in the UV chromosomes of the brown algae *Ectocarpus* (Ahmed et al. 2014). Alternatively, it could also be due to the lack of information about the ancestral gene order on the mating type (Branco et al. 2017).

To counteract the effects of reduced recombination inside *MTs*, gene conversion between mating types has been suggested to act as a homogenizing force in *Chlamydomonas* (De Hoff et al. 2013). In fungal mating types, the suppression of recombination maintains linkage of mating-type genes within each locus, which is required for correct mating-type determination (Kües 2000; Branco et al. 2017). However, gene flow between mating type loci and gene conversion events have recently been reported in several species (Sun et al. 2012; Hartmann et al. 2020). This suggests an important difference in the evolutionary processes of

haploid sex determining systems versus diploid sex determining systems, where gene flow between sex determining regions is rare (Hartmann et al. 2020).

The diversification within Mamiellales is estimated to have occurred between 330 and 640 million years ago (Lang et al. 2010)(Blank 2013)(Parfrey et al. 2011), much earlier than the diversification within Volvocales where deep homology of mating type loci has been reported (Ferris et al. 2010), and with a higher upper limit to the estimated 370 million years divergence of the STE3-like pheromone receptors from basidiomycete fungi (Devier et al. 2009). Therefore, our data suggest the Mamiellales mating type sex-determining region to be among the oldest mating type reported.

In conclusion**,** we analysed the phylogenetic profiles of the gene families within the *Ostreococcus* mating types, and gained insights into the evolutionary history of this sex-determining region in one of the earliest diverging orders of Chlorophytes. The identification of strains from the two opposite mating types in three species will guide future experimental approaches for mating and strain crossing, since a highly efficient transformation protocol is now available in *Ostreococcus* (Sanchez et al. 2019). Complete genome sequences in additional Mamiellophyceae are now essential to investigate the early dynamics of the sex-determining regions in the green lineage.

Materials and Methods

Mating type gene family definition

The full set of predicted genes from eight Mamelliales genomes (supplementary table S1, Supplementary Material online) was loaded into a custom version of the pico-PLAZA framework (Proost et al. 2009; Vandepoele et al. 2013) to define and analyse gene families (GFs). Following an 'all-against-all' protein sequence similarity search, performed with BLASTP (version 2.6.0+, maximum E-value threshold 1e-4, keeping up to 2,500 hits), we delineated GFs using OrthoFinder version 2.1.2 (Emms and Kelly 2015).

The boundaries of the mating type (*MT*) region of *Ostreococcus tauri* RCC4221 and RCC1115 served as a starting point for defining candidate *MT* GFs (supplementary table S1, Supplementary Material online). All genes located within either *MT* region were extracted, based on the coordinates of their coding sequence (CDS). For each gene included in these two gene sets, the GF they were assigned to was subsequently retrieved, consisting of a validated homologous group of ortholog and paralog genes in eight available genomes. Based on the location of the GF members (chromosome or scaffold and coordinates), a '*MT* signal' value

was then computed for every genome in which the GF was represented. This value corresponds to the fraction of members located within the *MT* region (for the given genome-GF combination), and was used to filter and classify the list of candidate GFs. The complete list of *MT* GFs is reported in supplementary table S9, Supplementary Material online.

For every retained GF, protein sequences were aligned using MAFFT version 7.187 (Katoh and Standley 2013) with the L-INS-i alignment method and a maximum of 1,000 iterative refinements. We edited the multiple sequence alignments (MSAs) using several filters on both sequences and positions, implemented in the PLAZA framework and described by Proost (Proost et al. 2009). Briefly, highly divergent and partial sequences were filtered out, and positions containing gaps in minimum 10% of the sequences or containing potentially misaligned amino acids removed. We also applied a minimum length cut-off to the edited MSA: the edited MSA had to be 50-amino-acid-long at least, otherwise we ignored it. In case the original unedited MSA was shorter, we used this length as a cut-off value instead. Finally, we retained only MSAs that showed at least 50% alignment of amino-acid identity in half of the sequences of the MSA. The circular plots depicting the location of homologous genes from GFs having copies outside of the *O. tauri MT* loci (fig. 2B and 2C) were generated with the circlize package in R (Gu et al. 2014; https://r-project.org/).

To test different gene order rearrangement scenarios between the *MT+* and *MT-* regions, we defined S_{dist}, which is the absolute value of the difference of the position of orthologous genes on the MT+ and MT- regions. If there are n orthologous genes between the two loci with pi- the position (in rank) of gene i on MT- and pi+ the position of its ortholog on MT+, $S_{dist} = \sum_{i=1}^{n} |p_{i-} - p_{i+}|$. S_{dist}=0 if all orthologs are perfectly collinear. The expected S_{dist} under random position of orthologous genes in the two mating types was assessed by simulations. If there has been an inversion of gene order between the two regions, S_{dist} is maximal, $S_{dist}=z(2n-2z)$, with $z=n/2$ if n is even, and $z=(n-1)/2$ if z is odd.

Gene family clustering and phylogeny

For each GF MSA that passed our filtering criteria, we built a Maximum Likelihood (ML) phylogenetic tree using IQ-TREE version 1.6.5 (Nguyen et al. 2015). Trees were built under the best-fitting substitution model selected by ModelFinder (Kalyaanamoorthy et al. 2017), chosen among commonly used models (JTT, LG, WAG, Blosum62, VT, and Dayhoff). Empirical amino-acid frequencies were calculated from the data, the FreeRate model (Yang 1995; Soubrier et al. 2012) was used to account for rate heterogeneity across sites, and branch

supports were assessed using ultrafast bootstrap approximation (UFBoot) (Soubrier et al. 2012) with 1,000 bootstrap replicates.

We used similar alignment, MSA editing, and phylogenetic tree building procedures when considering sequences from external sources (e.g. transcripts from MMETSP samples). The divergent gene removal criterion was based on the results of the all-against-all protein sequence similarity search performed using data from the eight reference genomes only (supplementary table S1, Supplementary Material online). Therefore, it was not used to filter out these sequences from the MSAs. Phylogenetic trees were built for full alignments in case the editing was deemed too stringent, for instance discarding transcripts flagged as partial sequences. Finally, when investigating the molecular phylogeny of the 18S rDNA genes, we used IQ-TREE's ModelFinder Plus parameter to select the best DNA substitution model.

Gene family phylogenetic tree classification

We visualised and inspected the *MT* GF trees using FigTree version 1.4.4 (http://tree.bio.ed.ac.uk/software/figtree/). We examined ultrafast bootstrap support values and topology type, and counted the number of times genes clustered by mating type or according to their taxonomic classification (by species).

Searching for homologs in publicly available transcriptomes

We used sequences of core *MT* GF members as queries to search for homologs in Mamiellophyceae transcriptomes (33 transcriptomes in total, listed in supplementary table S5, Supplementary Material online). Transcriptomes were retrieved from the MMETSP (Keeling et al. 2014; Johnson et al. 2019) and 1KP datasets (Matasci et al. 2014). Re-assembled MMETSP transcriptomes were downloaded from https://doi.org/10.5281/zenodo.251828 (version 1; January 2017) and 1KP transcriptomes via 1KP's R interface (https://github.com/ropensci/onekp). CDS from each Mamiellophyceae MMETSP transcriptome were predicted using TransDecoder (Haas et al. 2013) with default parameters. Sequence similarity searches were performed using tblastx (maximum E-value threshold 1e-4) and results were filtered to retain hits with alignment length > 50 and amino-acid identity > 60%. In-depth phylogenetic analyses of individual hits from *O. mediterraneus* strain RCC2572 (MMETSP0929), *O. lucimarinus* strain BCC118000 (MMETSP0939), *Micromonas* MMETSP transcriptomes (1084, 1327, 1387, 1393, 1400, 1401, 1402, 1403, 1404), and *Mantoniella* MMETSP transcriptomes (1106, 1468) were performed as previously described for the

reference genomes. The presence/absence matrix of each informative orthologous group against the transcriptomes was generated using the ggplot2 package in R) (Wickham 2011).

To validate and elucidate each MMETSP transcriptome's taxonomic affiliation, we downloaded Mamiellophyceae 18S rDNA sequences from reference genomes in GenBank, the SILVA database (Wickham 2011), and *Micromonas* spp. sequences provided in Simon et al. (2017) (supplementary table S6, Supplementary Material online). Transcripts matching selected 18S sequences were extracted with blastn (maximum E-value 1e-5) and 18S rDNA sequences were subsequently predicted using RNammer (Lagesen et al. 2007). A ML phylogenetic tree was built using IQ-TREE and following each clustering of this Mamiellophyceae reference tree (rooted in *Monomastix* spp.), transcriptomes were tentatively classified according to a species clustering (supplementary fig. S2, Supplementary Material online). Phylogeny indicated that MMETSP transcriptomes matched their species classification, and transcriptomes from novel *Micromonas* species as *M. polaris* and *M. bravo* were designated using the data and new classification of (Simon et al. 2017).

Compositional analysis (GC3) of gene families in Mamiellophyceae

To evaluate compositional differences between third codon positions (GC3) of GF members and CDS from the overall genome or transcriptome (supplementary table S8, Supplementary Material online) we used a custom python script to perform GC3 calculations. We subsequently evaluated the results using Student's *t*-test as implemented in R.

Synonymous and non-synonymous divergence of shared *MT* gene families

We used homologous pairs of the 69 shared *MT* GFs to calculate sequence genetic divergence with the seqinr package v3.4-5 (kaks function) using (Li 1993) method (LWL85) in R.

Acknowledgements

This work was funded by the European Union's Horizon 2020 research and innovation programme under the Marie Skłodowska-Curie ITN project SINGEK (H2020-MSCA-ITN-2015-675752 to L.F.B. and F.B.). We thank the Moore foundation for sequencing most of the Mamiellophycean transcriptomes analysed in this study and the Genotoul Bioinformatic platform for providing computing and data storage resources.

Data availability statement

All genomic and transcriptomic sequence data is available on GenBank under accession number CAID00000000.1 (O. tauri), PRJNA337288 (O. lucimarinus), PRJNA15676 (M. commoda),

PRJNA15678 (M. pusilla), PRJNA394752 (B. prasinos), PRJNA248394 (MMESTP). The accession numbers of the 18S rDNA sequences are summarized in Supplemental Table S6.

References

Ahmed S, Cock JM, Pessia E, Luthringer R, Cormier A, Robuchon M, Sterck L, Peters AF, Dittami SM, Corre E, et al. 2014. A haploid system of sex determination in the brown alga Ectocarpus sp. Curr. Biol. CB 24:1945–1957.

Astell CR, Ahlstrom-Jonasson L, Smith M, Tatchell K, Nasmyth KA, Hall BD. 1981. The sequence of the DNAs coding for the mating-type loci of *Saccharomyces cerevisiae*. Cell 27:15–23.

Bachtrog D, Kirkpatrick M, Mank JE, McDaniel SF, Pires JC, Rice W, Valenzuela N. 2011. Are all sex chromosomes created equal? Trends Genet. 27:350–357.

Bachtrog D, Mank JE, Peichel CL, Kirkpatrick M, Otto SP, Ashman T-L, Hahn MW, Kitano J, Mayrose I, Ming R, et al. 2014. Sex determination: why so many ways of doing it? PLoS Biol. 12:e1001899.

Badouin H, Hood ME, Gouzy J, Aguileta G, Siguenza S, Perlin MH, Cuomo CA, Fairhead C, Branca A, Giraud T. 2015. Chaos of Rearrangements in the Mating-Type Chromosomes of the Anther-Smut Fungus Microbotryum lychnidis-dioicae. Genetics 200:1275.

Beutlich A, Schnetter R. 1993. The Life Cycle of Cryptochlora perforans (Chlorarachniophyta). Bot. Acta 106:441–447.

Billiard S, López-Villavicencio M, Devier B, Hood ME, Fairhead C, Giraud T. 2011. Having sex, yes, but with whom? Inferences from fungi on the evolution of anisogamy and mating types. Biol. Rev. Camb. Philos. Soc. 86:421–442.

Billiard S, López-Villavicencio M, Hood ME, Giraud T. 2012. Sex, outcrossing and mating types: unsolved questions in fungi and beyond. J. Evol. Biol. 25:1020–1038.

Blanc-Mathieu R, Krasovec M, Hebrard M, Yau S, Desgranges E, Martin J, Schackwitz W, Kuo A, Salin G, Donnadieu C, Desdevises Y, Sanchez-Ferandin S, Moreau Hervé, et al. 2017. Population genomics of picophytoplankton unveils novel chromosome hypervariability. Sci. Adv. 3:e1700239.

Blanc-Mathieu R, Verhelst B, Derelle E, Rombauts S, Bouget F-Y, Carré I, Château A, Eyre-Walker A, Grimsley N, Moreau H, et al. 2014. An improved genome of the model marine alga Ostreococcus tauri unfolds by assessing Illumina de novo assemblies. BMC Genomics 15:1103.

Blank CE. 2013. Origin and early evolution of photosynthetic eukaryotes in freshwater environments: reinterpreting proterozoic paleobiology and biogeochemical processes in light of trait evolution. J. Phycol. 49:1040–1055.

Branco S, Badouin H, Rodríguez de la Vega RC, Gouzy J, Carpentier F, Aguileta G, Siguenza S, Brandenburg J-T, Coelho MA, Hood ME, et al. 2017. Evolutionary strata on young mating-type chromosomes despite the lack of sexual antagonism. Proc. Natl. Acad. Sci. 114:7067.

Charlesworth B, Charlesworth D. 2000. The degeneration of Y chromosomes. Philos. Trans. R. Soc. B Biol. Sci. 355:1563–1572.

Charlesworth D. 2016. Plant Sex Chromosomes. Annu. Rev. Plant Biol. 67:397–420.

Charlesworth D, Zhang Y, Bergero R, Graham C, Gardner J, Yong L. 2020. Using GC Content to Compare Recombination Patterns on the Sex Chromosomes and Autosomes of the Guppy, Poecilia reticulata, and Its Close Outgroup Species. Mol. Biol. Evol. [Internet].

Chepurnov VA, Mann DG, Sabbe K, Vyverman W. 2004. Experimental studies on sexual reproduction in diatoms. Int. Rev. Cytol. 237:91–154.

Coelho SM, Gueno J, Lipinska AP, Cock JM, Umen JG. 2018. UV Chromosomes and Haploid Sexual Systems. Trends Plant Sci. 23:794–807.

De Hoff PL, Ferris P, Olson BJSC, Miyagi A, Geng S, Umen JG. 2013. Species and population level molecular profiling reveals cryptic recombination and emergent asymmetry in the dimorphic mating locus of C. reinhardtii. PLoS Genet. 9:e1003724.

Derelle E, Ferraz C, Rombauts S, Rouze P, Worden AZ, Robbens S, Partensky F, Degroeve S, Echeynie S, Cooke R, et al. 2006. Genome analysis of the smallest free-living eukaryote Ostreococcus tauri unveils many unique features. Proc Natl Acad Sci U A 103:11647–11652.

Devier B, Aguileta G, Hood ME, Giraud T. 2009. Ancient Trans-specific Polymorphism at Pheromone Receptor Genes in Basidiomycetes. Genetics 181:209–223.

Ebenezer TE, Zoltner M, Burrell A, Nenarokova A, Novák Vanclová AMG, Prasad B, Soukal P, Santana-Molina C, O'Neill E, Nankissoor NN, et al. 2019. Transcriptome, proteome and draft genome of Euglena gracilis. BMC Biol. 17:11.

Emms DM, Kelly S. 2015. OrthoFinder: solving fundamental biases in whole genome comparisons dramatically improves orthogroup inference accuracy. Genome Biol. 16:157.

Ferris P, Olson BJSC, De Hoff PL, Douglass S, Casero D, Prochnik S, Geng S, Rai R, Grimwood J, Schmutz J, et al. 2010. Evolution of an expanded sex-determining locus in Volvox. Science 328:351–354.

Ferris PJ, Armbrust EV, Goodenough UW. 2002. Genetic structure of the mating-type locus of Chlamydomonas reinhardtii. Genetics 160:181–200.

Ferris PJ, Goodenough UW. 1997. Mating type in Chlamydomonas is specified by mid, the minus-dominance gene. Genetics 146:859–869.

Fontanillas E, Hood ME, Badouin H, Petit E, Barbe V, Gouzy J, de Vienne DM, Aguileta G, Poulain J, Wincker P, et al. 2015. Degeneration of the nonrecombining regions in the mating-type chromosomes of the anther-smut fungi. Mol. Biol. Evol. 32:928–943.

Fučíková K, Pažoutová M, Rindi F. 2015. Meiotic genes and sexual reproduction in the green algal class Trebouxiophyceae (Chlorophyta). J. Phycol. 51:419–430.

Galtier N, Piganeau G, Mouchiroud D, Duret L. 2001. GC-content evolution in mammalian genomes: the biased gene conversion hypothesis. Genetics 159:907–911.

Geng S, Miyagi A, Umen JG. 2018. Evolutionary divergence of the sex-determining gene MID uncoupled from the transition to anisogamy in volvocine algae. Dev. Camb. Engl. 145.

Grimsley N, Péquin B, Bachy C, Moreau H, Piganeau G. 2010. Cryptic sex in the smallest eukaryotic marine green alga. Mol. Biol. Evol. 27:47–54.

Gu Z, Gu L, Eils R, Schlesner M, Brors B. 2014. circlize Implements and enhances circular visualization in R. Bioinforma. Oxf. Engl. 30:2811–2812.

Haas BJ, Papanicolaou A, Yassour M, Grabherr M, Blood PD, Bowden J, Couger MB, Eccles D, Li B, Lieber M, et al. 2013. De novo transcript sequence reconstruction from RNA-Seq: reference generation and analysis with Trinity. Nat. Protoc. [Internet] 8. Available from: https://www.ncbi.nlm.nih.gov/pmc/articles/PMC3875132/

Hadjivasiliou Z, Pomiankowski A. 2016. Gamete signalling underlies the evolution of mating types and their number. Philos. Trans. R. Soc. Lond. B. Biol. Sci. 371.

Hamaji T, Kawai-Toyooka H, Uchimura H, Suzuki M, Noguchi H, Minakuchi Y, Toyoda A, Fujiyama A, Miyagishima S, Umen JG, et al. 2018. Anisogamy evolved with a reduced sex-determining region in volvocine green algae. Commun. Biol. 1:17.

Hamaji T, Mogi Y, Ferris PJ, Mori T, Miyagishima S, Kabeya Y, Nishimura Y, Toyoda A, Noguchi H, Fujiyama A, et al. 2016. Sequence of the Gonium pectorale Mating Locus Reveals a Complex and Dynamic History of Changes in Volvocine Algal Mating Haplotypes. G3 GenesGenomesGenetics 6:1179–1189.

Hartmann FE, Duhamel M, Carpentier F, Hood ME, Foulongne-Oriol M, Silar P, Malagnac F, Grognet P, Giraud T. 2021. Recombination suppression and evolutionary strata around mating-type loci in fungi: documenting patterns and understanding evolutionary and mechanistic causes. New Phytol. 229:2470–2491.

Hartmann FE, Rodríguez de la Vega RC, Gladieux P, Ma W-J, Hood ME, Giraud T. 2020. Higher Gene Flow in Sex-Related Chromosomes than in Autosomes during Fungal Divergence. Mol. Biol. Evol. 37:668–682.

Hill DRA, Wetherbee R. 1986. Proteomonas sulcata gen. et sp. nov. (Cryptophyceae), a cryptomonad with two morphologically distinct and alternating forms. Phycologia 25:521–543.

Hoekstra RF. 1987. The evolution of sexes. Experientia. Suppl. 55:59–91.

Hurst LD, Hamilton WD. 1992. Cytoplasmic fusion and the nature of sexes. Proc. R. Soc. Lond. B Biol. Sci. 247:189–194.

Jain A, Perisa D, Fliedner F, von Haeseler A, Ebersberger I. 2019. The Evolutionary Traceability of a Protein. Genome Biol. Evol. 11:531–545.

Jancek S, Gourbière S, Moreau H, Piganeau G. 2008. Clues about the genetic basis of adaptation emerge from comparing the proteomes of two Ostreococcus ecotypes (Chlorophyta, Prasinophyceae). Mol. Biol. Evol. 25:2293–2300.

Johnson LK, Alexander H, Brown CT. 2019. Re-assembly, quality evaluation, and annotation of 678 microbial eukaryotic reference transcriptomes. GigaScience [Internet] 8. Available from: https://academic.oup.com/gigascience/article/8/4/giy158/5241890

Joli N, Monier A, Logares R, Lovejoy C. 2017. Seasonal patterns in Arctic prasinophytes and inferred ecology of Bathycoccus unveiled in an Arctic winter metagenome. ISME J. 11:1372–1385.

Kalyaanamoorthy S, Minh BQ, Wong TKF, von Haeseler A, Jermiin LS. 2017. ModelFinder: fast model selection for accurate phylogenetic estimates. Nat. Methods 14:587–589.

Katoh K, Standley DM. 2013. MAFFT Multiple Sequence Alignment Software Version 7: Improvements in Performance and Usability. Mol. Biol. Evol. 30:772–780.

Keeling PJ, Burki F, Wilcox HM, Allam B, Allen EE, Amaral-Zettler LA, Armbrust EV, Archibald JM, Bharti AK, Bell CJ, et al. 2014. The Marine Microbial Eukaryote Transcriptome Sequencing Project (MMETSP): illuminating the functional diversity of eukaryotic life in the oceans through transcriptome sequencing. PLoS Biol. 12:e1001889.

Krasovec M, Eyre-Walker A, Sanchez-Ferandin S, Piganeau G. 2017. Spontaneous Mutation Rate in the Smallest Photosynthetic Eukaryotes. Mol. Biol. Evol. 34:1770–1779.

Kües U. 2000. Life history and developmental processes in the basidiomycete Coprinus cinereus. Microbiol. Mol. Biol. Rev. MMBR 64:316–353.

Kugrens P, Lee RE. 1988. Ultrastructure of Fertilization in a Cryptomonad1. J. Phycol. 24:385–393.

Kumar S, Stecher G, Suleski M, Hedges SB. 2017. TimeTree: A Resource for Timelines, Timetrees, and Divergence Times. Mol. Biol. Evol. 34:1812–1819.

Lahn BT, Page DC. 1999. Four evolutionary strata on the human X chromosome. Science 286:964–967.

Lang D, Weiche B, Timmerhaus G, Richardt S, Riaño-Pachón DM, Corrêa LGG, Reski R, Mueller-Roeber B, Rensing SA. 2010. Genome-wide phylogenetic comparative analysis of plant transcriptional regulation: a timeline of loss, gain, expansion, and correlation with complexity. Genome Biol. Evol. 2:488–503.

Leconte J, Benites LF, Vannier T, Wincker P, Piganeau G, Jaillon O. 2020. Genome Resolved Biogeography of Mamiellales. Genes 11:66.

Lengeler KB, Fox DS, Fraser JA, Allen A, Forrester K, Dietrich FS, Heitman J. 2002. Mating-Type Locus of Cryptococcus neoformans: a Step in the Evolution of Sex Chromosomes. Eukaryot. Cell 1:704–718.

Li W-H. 1993. Unbiased estimation of the rates of synonymous and nonsynonymous substitution. J. Mol. Evol. 36:96–99.

Ma W-J, Carpentier F, Giraud T, Hood ME. 2020. Differential Gene Expression between Fungal Mating Types Is Associated with Sequence Degeneration. Genome Biol. Evol. 12:243–258.

Malik S-B, Ramesh MA, Hulstrand AM, Logsdon JM. 2007. Protist homologs of the meiotic Spo11 gene and topoisomerase VI reveal an evolutionary history of gene duplication and lineage-specific loss. Mol. Biol. Evol. 24:2827–2841.

Matasci N, Hung L-H, Yan Z, Carpenter EJ, Wickett NJ, Mirarab S, Nguyen N, Warnow T, Ayyampalayam S, Barker M, et al. 2014. Data access for the 1,000 Plants (1KP) project. GigaScience 3:17.

McKim KS, Howell AM, Rose AM. 1988. The effects of translocations on recombination frequency in Caenorhabditis elegans. Genetics 120:987–1001.

Meunier J, Duret L. 2004. Recombination drives the evolution of GC-content in the human genome. Mol Biol Evol 21:984–990.

Natri HM, Merilä J, Shikano T. 2019. The evolution of sex determination associated with a chromosomal inversion. Nat. Commun. 10:145.

Nguyen L-T, Schmidt HA, von Haeseler A, Minh BQ. 2015. IQ-TREE: a fast and effective stochastic algorithm for estimating maximum-likelihood phylogenies. Mol. Biol. Evol. 32:268–274.

Nozaki H, Mori T, Misumi O, Matsunaga S, Kuroiwa T. 2006. Males evolved from the dominant isogametic mating type. Curr. Biol. 16:R1018–R1020.

Palenik B, Grimwood J, Aerts A, Rouze P, Salamov A, Putnam N, Dupont C, Jorgensen R, Derelle E, Rombauts S, et al. 2007. The tiny eukaryote Ostreococcus provides genomic insights into the paradox of plankton speciation. Proc Natl Acad Sci U A 104:7705–7710.

Parfrey LW, Lahr DJG, Knoll AH, Katz LA. 2011. Estimating the timing of early eukaryotic diversification with multigene molecular clocks. Proc. Natl. Acad. Sci. 108:13624–13629.

Pfiester LA. 1989. Dinoflagellate Sexuality. In: Bourne GH, Jeon KW, Friedlander M, editors. International Review of Cytology. Vol. 114. Academic Press. p. 249–272.

Proost S, Bel MV, Sterck L, Billiau K, Parys TV, Peer YV de, Vandepoele K. 2009. PLAZA: A Comparative Genomics Resource to Study Gene and Genome Evolution in Plants. Plant Cell 21:3718–3731.

Richman A. 2000. Evolution of balanced genetic polymorphism. Mol. Ecol. 9:1953–1963.

Sager R, Granick S. 1954. Nutritional control of sexuality in Chlamydomonas reinhardi. J. Gen. Physiol. 37:729–742.

Sanchez F, Geffroy S, Norest M, Yau S, Moreau H, Grimsley N. 2019. Simplified Transformation of Ostreococcus tauri Using Polyethylene Glycol. Genes 10.

Slapeta J, Lopez-Garcia P, Moreira D. 2006. Global dispersal and ancient cryptic species in the smallest marine eukaryotes. Mol Biol Evol 23:23–29.

Sonneborn TM. 1937. Sex, Sex Inheritance and Sex Determination in Paramecium Aurelia. Proc. Natl. Acad. Sci. U. S. A. 23:378–385.

Soubrier J, Steel M, Lee MSY, Der Sarkissian C, Guindon S, Ho SYW, Cooper A. 2012. The Influence of Rate Heterogeneity among Sites on the Time Dependence of Molecular Rates. Mol. Biol. Evol. 29:3345–3358.

Speijer D, Lukes J, Elias M. 2015. Sex is a ubiquitous, ancient, and inherent attribute of eukaryotic life. Proc. Natl. Acad. Sci. U. S. A. 112:8827–8834.

Staben C, Yanofsky C. 1990. Neurospora crassa a mating-type region. Proc. Natl. Acad. Sci. 87:4917–4921.

Strehlow, K. 1929. Über die Sexualität einiger Volvocales. Zeitschrift für Botanik 21:625:692.

Suda S, Watanabe MM, Inouye I. 1989. Evidence for Sexual Reproduction in the Primitive Green Alga Nephroselmis Olivacea (prasinophyceae)1. J. Phycol. 25:596–600.

Sun Y, Corcoran P, Menkis A, Whittle CA, Andersson SGE, Johannesson H. 2012. Large-Scale Introgression Shapes the Evolution of the Mating-Type Chromosomes of the Filamentous Ascomycete Neurospora tetrasperma. PLOS Genet. 8:e1002820.

Tzeng Y-H, Pan R, Li W-H. 2004. Comparison of three methods for estimating rates of synonymous and nonsynonymous nucleotide substitutions. Mol. Biol. Evol. 21:2290–2298.

Umen J, Coelho S. 2019. Algal Sex Determination and the Evolution of Anisogamy. Annu. Rev. Microbiol. 73:267–291.

Umen JG. 2011. Evolution of sex and mating loci: an expanded view from Volvocine algae. Curr. Opin. Microbiol. 14:634–641.

Vandepoele K, Bel MV, Richard G, Landeghem SV, Verhelst B, Moreau H, Peer YV de, Grimsley N, Piganeau G. 2013. pico-PLAZA, a genome database of microbial photosynthetic eukaryotes. Environ. Microbiol. 15:2147–2153.

Wang L, Berndt P, Xia X, Kahnt J, Kahmann R. 2011. A seven-WD40 protein related to human RACK1 regulates mating and virulence in Ustilago maydis. Mol. Microbiol. 81:1484–1498.

Wickham H. 2011. ggplot2. WIREs Comput. Stat. 3:180–185.

Wilson AM, Wilken PM, van der Nest MA, Wingfield MJ, Wingfield BD. 2019. It's All in the Genes: The Regulatory Pathways of Sexual Reproduction in Filamentous Ascomycetes. Genes 10.

Wolfe KH, Butler G. 2017. Evolution of Mating in the Saccharomycotina. Annu. Rev. Microbiol. 71:197–214.

Worden AZ, Lee JH, Mock T, Rouze P, Simmons MP, Aerts AL, Allen AE, Cuvelier ML, Derelle E, Everett MV, et al. 2009. Green evolution and dynamic adaptations revealed by genomes of the marine picoeukaryotes Micromonas. Science 324:268–272.

Yamamoto K, Hamaji T, Kawai-Toyooka H, Matsuzaki R, Takahashi F, Nishimura Y, Kawachi M, Noguchi H, Minakuchi Y, Umen JG, et al. 2021. Three genomes in the algal genus *Volvox* reveal the fate of a haploid sex-determining region after a transition to homothallism. Proc. Natl. Acad. Sci. 118:e2100712118.

Yang Z. 1995. A space-time process model for the evolution of DNA sequences. Genetics 139:993–1005.

List of Figure Legends

Figure 1: Size and GC content in the candidate mating type chromosomes (candidate mating type locus positions as in Sup. Table S1) in the 8 Mamiellales genomes. Sequences of CH02 of O. lucimarinus and M. pusilla have been reversed complemented to take colinearity of flanking regions as described in (Palenik et al. 2007) and (Worden et al. 2009) into account. Node divergence estimations are from (Slapeta et al. 2006) for Micromonas and (Parfrey et al. 2011) for the basal node.

Figure 2: Gene organization in the mating type region of *O. tauri* RCC4221 (*MT*-) and RCC1115 (*MT*+). (**A**) Location of gene pairs from the 23 core gene families (GFs) and 57 shared GFs in the mating type region of *O. tauri* RCC4221 (*MT*-, blue rectangle) and RCC1115 (*MT*+, red rectangle). Genes from core and shared GFs are represented by bright and dark ticks, respectively, and homologous gene pairs are connected by grey lines. Genes from *MT*+ or *MT*- specific GFs are also shown, represented by black ticks. Shared gene families having multiple copies in either *O. tauri* RCC4221 (*MT*-) and RCC1115 (*MT*+) are not depicted. (**B, C**) Location of homologous *MT* genes from GFs with copies outside of either *O. tauri MT* region in Mamiellales genomes, for *O. tauri* RCC4221 (*MT*-, 39 GFs, **B**) and RCC1115 (*MT*+, 16 GFs, **C**). Each peripheral segment represents a chromosome or scaffold of one of eight Mamiellales genomes. The *MT* genes from *O. tauri* RCC4221 (*MT*-, **B**) or RCC1115 (*MT*+, **C**) are connected to their homologs by grey lines. If a homolog is located within a *MT* locus, the link is coloured in orange. The abbreviations are as follows: chromosome (CH), contig (CG), and unitig (UG).

Figure 3: Phylogenetic signal and GC3 content of gene family (GF) members in *O. tauri* RCC4221 (*MT*-) and RCC1115 (*MT*+). 'Post' for GF genes with mating type separation after speciation and 'Ante' for GF genes with mating type separation prior to speciation. Circle size is proportional to the number of GF genes (numerical value within each circle), and circle colour depicts the average GC3 content from low (yellow-golden) to high (green).

Figure 4: Unrooted maximum-likelihood phylogenetic trees of representative core *MT* gene families 000581 (**A**) and 000945 (**B**). Genes from *MT*- strains are coloured in blue, genes from *MT*+ strains are coloured in red. Ultrafast bootstrap support values are denoted on branches. Abbreviations: *O. tauri* RCC4221 (OT4221), *O. tauri* RCC1115 (OT1115), *O. lucimarinus*

(OL), *O*. sp RCC809 (O809), *O*. *mediterraneus* RCC2590 (OMED), *B. prasinos* RCC1105 (B1105), *M. commoda* RCC299 (MC299), and *M*. *pusilla* (MPU).

Figure 5: Presence-absence matrix of best BLAST hits (BBH) of core *MT* gene families in each Mamiellophyceae transcriptome. Species' names of sequenced strains (left column) as inferred from 18S rDNA sequence analysis extracted from the transcriptome (supplementary fig. S2, Supplementary Material online). The colour of each rectangle indicates the taxonomic affiliation of the BBH (colour key at the bottom). Transcriptomes containing genes with a BBH affiliated to a different species are highlighted in grey.

Figure 6: Unrooted maximum-likelihood phylogenetic trees of representative core *MT* gene families 001374 (**A**) and 003390 (**B**) including homologous sequences from *O. lucimarinus* MMETSP0939 (strain BCC118000) and *O. mediterraneus* MMETSP0929 (strain RCC2572). Candidate mating type genes *MT*+ are in red, *MT*- in blue. Topology (**A**) clusters genes according to mating type, whereas topology (**B**) corresponds to the species phylogeny. Ultrafast bootstrap support values are indicated on branches. Abbreviations: *O*. *tauri* RCC4221 (OT4221), *O*. *tauri* RCC1115 (OT1115), *O*. *lucimarinus* (OL), *O*. *lucimarinus* BCC118000 (OLMMETSP0939), *O*. sp RCC809 (O809), *O*. *mediterraneus* RCC2590 (OMED), *O*. *mediterraneus* RCC2572 (OMMMETSP0929), *B. prasinos* RCC1105 (B1105), *M. commoda* RCC299 (MC299), and *M*. *pusilla* (MPU).

Figure 7: Phylogenetic trees of representative core *MT* gene families 001102 (**A**) and 003908 **(C)**, and actin (**B**) and β-tubulin (**D**) genes, for *M. commoda* and *M*. *pusilla* reference genomes and homologous genes retrieved from diverse *Micromonas* spp. transcriptomes. In the phylogeny "A", two *M*. *commoda* sub-clusters are highlighted in dark green (MMETSP1403, 1400, 1084, 1387) and light green (MMETSP1393, 1404, and the reference *M*. *commoda* RCC299). In phylogeny "C", there is no "A type" sub-clustering. In the actin and β-tubulin trees, sub-clusters are absent and branch lengths are shorter than "A", but parallel with phylogeny "C".

Figure 8: GC3 content comparison between genes from core *MT* gene families (dark green) and overall genome or transcriptome (light green) in Mamiellophyceae species. Phylogenetic relationships are inferred from 18S rDNA phylogeny. An asterisk (*) indicates a significant GC3 content difference (Student's *t*-test p-value < 0.05). Abbreviations: *O*. *tauri* RCC4221

(*Ostreococcus*), *B. prasinos* RCC1105 (*Bathycoccus*), *M. pusilla* CCMP1545 (*Micromonas*), *M. squamata* strain CCMP1436 - MMETSP1468 (*Mantoniella squamata*), *M. squamata* strain CCCAP 1965/1 - QXSZ (*M. squamata*), *M. antarctica* strain SL-175 - MMETSP1106 (*Mantoniella antarctica*), Uncultured eukaryote RCC2288 - MMETSP1326 (Uncult. Mamiellophyceae), *C. stigmatica* CCMP3273 - MMETSP0803 (*Crustomastix*), *D. tenuilepis* CCMP3274 - MMETSP0033 (*Dolichomastix*), *D. tenuilepis* strain M1680 - XOAL (*D. tenuilepis*), and *M. opisthostigma* CCAC 0206 - BTFM (*Monomastix*).

List of Tables

Table 1: Classification, description, and quantities of genes and gene families (GFs) in *O. tauri* RCC4221 *(MT-)* and RCC1115 (*MT+*) strains.

Table 1: Classification, description, and quantities of genes and gene families (GFs) in *O. tauri* RCC4221 *(MT-)* and RCC1115 (*MT+*) strains.

Gene Family class	Features of included genes	RCC4221 (*MT-*)	RCC1115 (*MT+*)
MT specific GFs	Present in either all *Ostreococcus MT-* or all *Ostreococcus MT+*	6 genes in 6 GFs	2 genes in 2 GFs
Core *MT* GFs	Present in all Mamiellales genomes and located only in *MT* region	23 genes in 23 GFs	23 genes in 23 GFs
Shared *MT* GFs (non-core)	Present in both *Ostreococcus MT* loci, but not in all Mamiellales *MT* regions	75 genes in 69 GFs	79 genes in 69 GFs
GFs extending outside *MT*	Present in one *Ostreococcus MT* locus but with homologous genes in other regions in the opposite strain	28 genes in 27 GFs	8 genes in 4 GFs
GFs not retained for analysis	Present in only one *Ostreococcus MT* locus and Mamiellales genomes but absent from the genomes of the opposite strains/*MT*; divergent GFs or singletons	112 genes	128 genes
Total number of genes		244	240

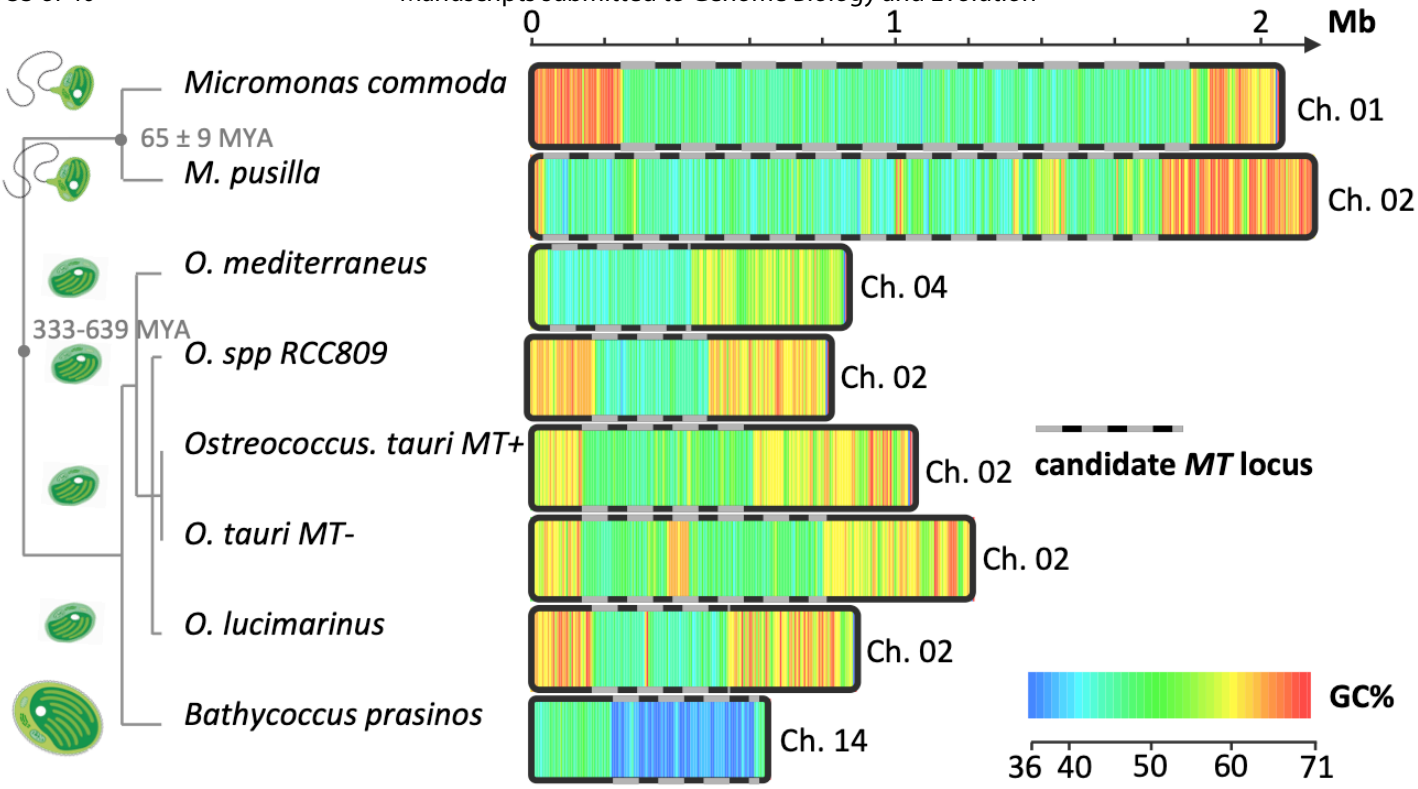

Figure 1. "Big Outlier Chromosome" size and GC content in eight completely sequences Mamiellales strains.

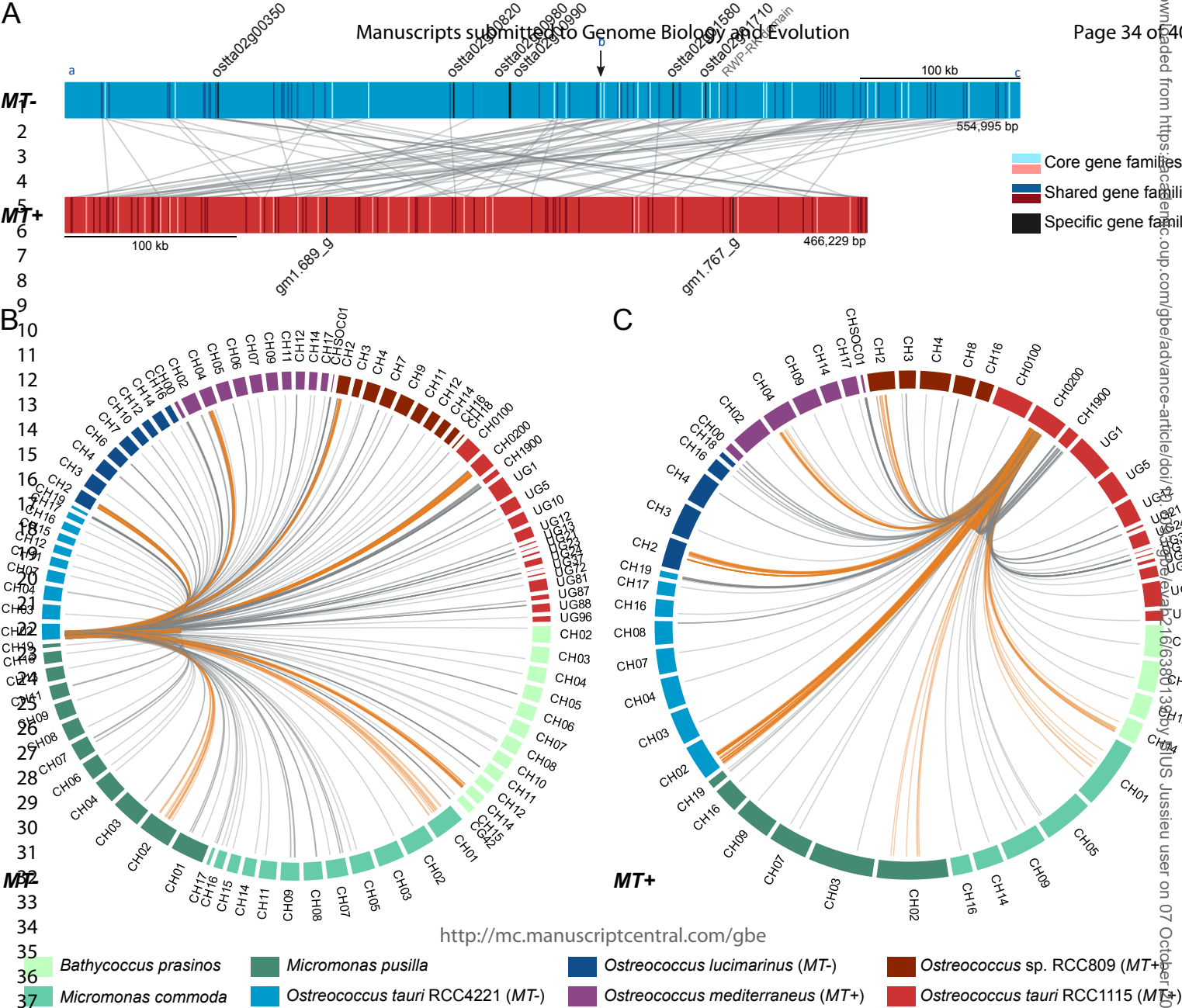

Manuscripts submitted to Genome Biology and Evolution